J|A|C|S
ARTICLES
Published on Web 09/06/2006

Dendrimer-Functionalized Single-Wall Carbon Nanotubes: Synthesis, Characterization, and Photoinduced Electron Transfer

Stéphane Campidelli,*,† Chloé Sooambar,† Enrique Lozano Diz,‡ Christian Ehli,§ Dirk M. Guldi,*,§ and Maurizio Prato*,†

Contribution from the INSTM and Dipartimento di Scienze Farmaceutiche, Università di Trieste, Piazzale Europa 1, 34127 Trieste, Italy, Instituto de Catalisis y Petroleoquimica, Campus de la Universidad Autonoma, C/ Marie Curie 2, 28049 Madrid, Spain, and Institute for Physical Chemistry, Friedrich-Alexander-Universität Erlangen-Nürnberg, Egerlandstrasse 3, 91058 Erlangen, Germany

Received May 26, 2006; E-mail: scampidelli@units.it; prato@units.it; guldi@chemie.uni-erlangen.de

Abstract: We describe the synthesis and characterization of a series of single-wall carbon nanotubes (SWNTs) functionalized with polyamidoamine dendrimers. Importantly, the dendrimers are linked directly to the SWNT surface using a divergent methodology. This approach allows the number of functional groups on the nanotubes to be increased without provoking significant damage to the conjugated π-system of the SWNTs. Several tetraphenylporphyrin moieties can be linked to the periphery of the dendrimers, and the photophysical properties of the resulting nanoconjugates have been investigated with a series of steady-state and time-resolved spectroscopy. The fluorescence kinetics provide evidence for two transient decays, one very short-lived (i.e., 0.04 ± 0.01 ns) and one long-lived (i.e., 8.6 ± 1.2 ns). A possible explanation is that some porphyrin units do not interact with the nanotubes, thus exhibiting a fluorescence lifetime similar to that of the free porphyrin. Complementary transient absorption measurements not only corroborate the fast decay of the photoexcited tetraphenylporphyrin but also confirm that intraconjugate charge separation evolves from the excited porphyrin to the SWNTs.

Introduction

During the past decade, nanometer-scale structures have attracted considerable attention within the scientific community.[1−3] Carbon nanotubes (CNTs)[4,5] constitute a relatively new class of nanostructures: they are composed exclusively of carbon atoms and possess exceptional mechanical, electronic, and optical properties. CNTs appear to be very promising materials for polymer composites,[6−9] energy conversion,[10−16] sensing,[17−19] or biological applications.[17,20−26] Single-wall carbon nanotubes (SWNTs) are one-dimensional nanowires that are either metallic or semiconducting. They readily accept charges, which can then be transported under nearly ideal conditions along the tubular SWNT axis.[27,28] The electrical conductivity, morphology, and

† Università di Trieste.
‡ Instituto de Catalisis y Petroleoquimica-CSIC.
§ Friedrich-Alexander-Universität Erlangen-Nürnberg.

(1) Poole, C. P.; Owens, F. J. *Introduction to Nanotechnology*; Wiley-Interscience: Weinheim, Germany, 2003.
(2) Liz-Marzán, L. M.; Kamat, P. V. *Nanoscale Materials*; Springer: Berlin, Germany, 2003.
(3) Wolf, E. L. *Nanophysics and Nanotechnology: An Introduction to Modern Concepts in Nanoscience*; John Wiley and Sons: New York, 2004.
(4) Dresselhaus, M. S.; Dresselhaus, G.; Avouris, P. *Carbon Nanotubes: Synthesis, Structure, Properties, and Applications*; Springer: Berlin, Germany, 2001.
(5) Reich, S.; Thomsen, C.; Maultzsch, J. *Carbon Nanotubes: Basic Concepts and Physical Properties*; VCH: Weinheim, Germany, 2004.
(6) Harris, P. J. F. *Int. Mater. Rev.* **2004**, *49*, 31.
(7) Chae, H. G.; Sreekumar, T. V.; Uchida, T.; Kumar, S. *Polymer* **2005**, *46*, 10925.
(8) Miyagawa, H.; Misra, M.; Mohanty, A. K. *J. Nanosci. Nanotechnol.* **2005**, *5*, 1593.
(9) Baibarac, M.; Gómez-Romero, P. *J. Nanosci. Nanotechnol.* **2006**, *6*, 289.
(10) Guldi, D. M.; Rahman, G. M. A.; Zerbetto, F.; Prato, M. *Acc. Chem. Res.* **2005**, *38*, 871.
(11) Rahman, G. M. A.; Guldi, D. M.; Cagnoli, R.; Mucci, A.; Schenetti, L.; Vaccari, L.; Prato, M. *J. Am. Chem. Soc.* **2005**, *127*, 10051.
(12) Guldi, D. M.; Rahman, G. M. A.; Sgobba, V.; Kotov, N. A.; Bonifazi, D.; Prato, M. *J. Am. Chem. Soc.* **2006**, *128*, 2315.
(13) Landi, B. J.; Castro, S. L.; Ruf, H. J.; Evans, C. M.; Bailey, S. G.; Raffaelle, R. P. *Sol. Energy Mater. Sol. Cells* **2005**, *87*, 733.
(14) Raffaelle, R. P.; Landi, B. J.; Harris, J. D.; Bailey, S. G.; Hepp, A. F. *Mater. Sci. Eng., B* **2005**, *116*, 233.
(15) Bhattacharyya, S.; Kymakis, E.; Amaratunga, G. A. J. *Chem. Mater.* **2004**, *16*, 4819.
(16) Ago, H.; Petritsch, K.; Shaffer, M. S. P.; Windle, A. H.; Friend, R. H. *Adv. Mater.* **1999**, *11*, 1281.
(17) Katz, E.; Willner, I. *ChemPhysChem* **2004**, *5*, 1084.
(18) Stampfer, C.; Helbling, T.; Obergfell, D.; Schoberle, B.; Tripp, M. K.; Jungen, A.; Roth, S.; Bright, V. M.; Hierold, C. *Nano Lett.* **2006**, *6*, 233.
(19) Sinha, N.; Ma, J. Z.; Yeow, J. T. W. *J. Nanosci. Nanotechnol.* **2006**, *6*, 573.
(20) Lin, Y.; Tailor, S.; Li, H.; Shiral Fernando, K. A.; Qu, L.; Wang, W.; Gu, L.; Zhou, B.; Sun, Y.-P. *J. Mater. Chem.* **2004**, *14*, 527.
(21) Bianco, A.; Kostaleros, K.; Partidos, C. D.; Prato, M. *Chem. Commun.* **2005**, 571.
(22) Wu, W.; Wieckowski, S.; Pastorin, G.; Benincasa, M.; Klumpp, C.; Briand, J.-P.; Gennaro, R.; Prato, M.; Bianco, A. *Angew. Chem., Int. Ed.* **2005**, *44*, 6358.
(23) Pastorin, G.; Wu, W.; Wieckowski, S.; Briand, J.-P.; Kostaleros, K.; Prato, M.; Bianco, A. *Chem. Commun.* **2006**, 1182.
(24) Singh, R.; Pantarotto, D.; Lacerda, L.; Pastorin, G.; Klumpp, C.; M. Prato, Bianco, A.; Kostaleros, K. *Proc. Natl. Acad. Sci. U.S.A.* **2006**, *103*, 3357.
(25) Kam, N. W. S.; O'Connell, M.; Wisdom, J. A.; Dai, H. *Proc. Natl. Acad. Sci. U.S.A.* **2005**, *102*, 11600.
(26) Kam, N. W. S.; Dai, H. *J. Am. Chem. Soc.* **2005**, *127*, 6021.

10.1021/ja063697i CCC: $33.50

good chemical stability of SWNTs are promising features that stimulate their integration into electronic devices.

However, processing SWNTs and integrating them into real world applications is severely limited by a number of inherent shortcomings: purification, manipulation, and low solubilities in organic solvents are some of them. To improve their solubility and overcome intertube aggregations, two general strategies have been explored in the recent past: (1) the covalent functionalization of sp^2 carbons at the sidewalls with organic pendant groups[29−37] and (2) the noncovalent functionalization through supramolecular interactions (e.g., $\pi-\pi$ stacking interactions), which allows the formation of stable suspensions.[10,20,38−42] It is generally admitted that extensive covalent functionalization of SWNT sidewalls disrupts the conjugated π-system of the tubes—affecting their optical and electronic properties. Therefore, weak functionalization processes might improve their processability while allowing the retention of the typical SWNT properties. In this context, functionalization of nanotubes with polymers and/or dendrimers represents a particularly promising strategy to attach a limited number of functional groups onto the SWNT surfaces without significantly disturbing the conjugated π-system.

While important work has demonstrated how to functionalize nanotubes with polymers, only a few examples where carbon nanotubes have been functionalized with dendrimers are known to date.[43−45] Dendrimers are very interesting macromolecules which possess a globular structure with a high density of functional groups on the periphery.[46−50]

With this goal in mind, we decided to build polyamidoamine (PAMAM) dendrimers directly onto SWNTs utilizing the nanotubes as a central core. PAMAM dendrimers, for instance, described by Tomalia[51] are relatively easy to synthesize. In particular, the divergent methodology, starting from ethylenediamine and methyl acrylate, leads to the desired target compounds. In this work we describe the synthesis of SWNTs functionalized with a second generation of PAMAM dendrimers (Scheme 1) as well as the derivatization of the terminal amino groups of the dendrons with tetraphenylporphyrins (Scheme 2). In the first step the SWNTs underwent a 1,3-dipolar cycloaddition reaction, which leads to the formation of a pyrrolidine ring functionalized with a *N-tert*-butoxycarbonyl (Boc)-protected amine group.[52,53] In the second step the dendrimers were built onto the nanotube surfaces.

Results and Discussion

The functionalized carbon nanotubes **1** were prepared by 1,3-dipolar cycloaddition among the amino acid **2**,[54] paraformaldehyde, and pristine HiPCO SWNTs in DMF. At the end of the reaction, the nanotubes were separated from the residue by filtration over a Millipore membrane (Fluoropore, 0.22 μm) and extensively washed with DMF, dichloromethane, and finally diethyl ether. The nanotubes were resuspended in DMF, and the Boc protecting group was removed by bubbling gaseous HCl through the suspension. The corresponding ammonium chloride salt **3** precipitated during the acid treatment and was recovered by filtration. The dendrimers were synthesized following a slightly modified procedure that was established for the solid-phase synthesis of PAMAM.[55] Methyl acrylate was added to a suspension of SWNTs **3** in methanol, and the resulting mixture was stirred at 80 °C for 3 days. The corresponding nanotubes **4** were separated by filtration, washed, dried, and then allowed to react with ethylenediamine to give SWNTs **5** grafted with first-generation PAMAM. The same reaction sequence led to the dendrimer of second-generation **7**. The amount of amine functions on compounds **3**, **5**, and **7** was determined by a quantitative Kaiser test.[56] We found a loading of amine groups of 63, 162, and 278 μmol·g^{-1} for **3**, **5**, and **7**, respectively. Finally, the coupling between 5,10,15-tris(3,5-di-*tert*-butylphenyl)-20-[4-(carbonyloxy)phenyl]porphyrin (**8**)[57,58] and the amine groups of the dendrimer in the presence of *N*-[3-(dimethylamino)propyl]-*N*′-ethylcarbodiimide (EDC) and 1-hydroxybenzotriazole (HOBt) gave SWNT−$(H_2P)_x$ nanoconjugates **9**. The nanotubes containing dendrimers **7** and **9** were sparingly soluble in DMF and *o*-dichlorobenzene.

The new compounds **1**, **7**, and **9** were fully characterized by standard analytical techniques, such as Raman spectroscopy, UV−vis−NIR spectroscopy, thermogravimetric analysis (TGA), transmission electron microscopy (TEM), and atomic force microscopy (AFM). The photophysical properties of **9** have also been investigated by steady-state and time-resolved fluorescence as well as femto- and nanosecond transient absorption.

FT-IR spectroscopy confirmed the presence of the carbonyl functions of the amide and/or ester groups in all compounds—except compound **3**. The IR spectrum of compound **1** shows a

(27) Javey, A.; Guo, J.; Wang, Q.; Lundstrom, M.; Dai, H. *Nature* **2003**, *424*, 654.
(28) Latil, S.; Roche, S.; Charlier, J.-C. *Nano Lett.* **2005**, *5*, 2216.
(29) Hirsch, A. *Angew. Chem., Int. Ed.* **2002**, *41*, 1853.
(30) Sun, Y.-P.; Fu, K.; Lin, Y.; Huang, W. *Acc. Chem. Res.* **2002**, *35*, 1096.
(31) Bahr, J.; Tour, J. M. *J. Mater. Chem.* **2002**, *12*, 1952.
(32) Niyogi, S.; Hamon, M. A.; Hu, H.; Zhao, B.; Bhowmik, P.; Sen, R.; Itkis, M. E.; Haddon, R. C. *Acc. Chem. Res.* **2002**, *35*, 1105.
(33) Banerjee, S.; Kanh, M. G. C.; Wong, S. S. *Chem.—Eur. J.* **2003**, *9*, 1899.
(34) Tasis, D.; Tagmatarchis, N.; Georgakilas, V.; Prato, M. *Chem.—Eur. J.* **2003**, *9*, 4000.
(35) Dyke, C. A.; Tour, J. M. *J. Phys. Chem. A* **2004**, *108*, 11151.
(36) Banerjee, S.; Hemraj-Benny, T.; Wong, S. S. *Adv. Mater.* **2005**, *17*, 17.
(37) Tasis, D.; Tagmatarchis, N.; Bianco, A.; Prato, M. *Chem. Rev.* **2006**, *106*, 1105.
(38) O'Connell, M. J.; Boul, P.; Ericson, L. M.; Huffman, C.; Wang, Y.; Haroz, E.; Kuper, C.; Tour, J.; Ausman, K. D.; Smalley, R. E. *Chem. Phys. Lett.* **2001**, *342*, 265.
(39) Star, A.; Stoddart, J. F.; Steuerman, D.; Diehl, M.; Boukai, A.; Wong, E. W.; Yang, X.; Chung, S.-W.; Choi, H.; Heath, J. R. *Angew. Chem., Int. Ed.* **2001**, *40*, 1721.
(40) Nakashima, N.; Tomonari, Y.; Murakami, H. *Chem. Lett.* **2002**, 638.
(41) Richard, C.; Balavoine, F.; Schultz, P.; Ebbesen, T. W.; Mioskowski, C. *Science* **2003**, *300*, 775.
(42) Numata, M.; Asai, M.; Kaneko, K.; Bae, A.-H.; Hasegawa, M.; Sakurai, K.; Shinkai, S. *J. Am. Chem. Soc.* **2005**, *127*, 5875.
(43) Sun, Y.-P.; Huang, W.; Lin, Y.; Fu, K.; Kitaygorodskiy, A.; Riddle, L. A.; Joy Yu, Y.; Caroll, D. L. *Chem. Mater.* **2001**, *13*, 2864.
(44) Holzinger, M.; Abraham, J.; Whelan, P.; Graupner, R.; Ley, L.; Hennrich, F.; Kappes, M.; Hirsch, A. *J. Am. Chem. Soc.* **2003**, *125*, 8566.
(45) Cao, L.; Yang, W.; Yang, J. W.; Wang, C. C.; Fu, S. K. *Chem. Lett.* **2004**, *33*, 490.
(46) Vögtle, F. *Dendrimers II Architecture, Nanostructure and Supramolecular Chemistry*; Springer: Berlin, Germany, 2000.
(47) Majoral, J.-P.; Caminade, A.-M. *Chem. Rev.* **1999**, *99*, 845.
(48) Bosman, A. W.; Janssen, H. M.; Meijer, E. W. *Chem. Rev.* **1999**, *99*, 1665.
(49) Newkome, G. R.; He, E.; Moorefield, C. N. *Chem. Rev.* **1999**, *99*, 1689.
(50) Grayson, S. M.; Fréchet, J. M. J. *Chem. Rev.* **2001**, *101*, 3819.
(51) Tomalia, D. A.; Baker, H.; Dewald, J. R.; Hall, M.; Kallos, G.; Martin, S.; Roeck, J.; Ryder, J.; Smith, P. *Polym. J.* **1985**, *17*, 117.
(52) Georgakilas, V.; Kordatos, K.; Prato, M.; Guldi, D. M.; Holzinger, M.; Hirsch, A. *J. Am. Chem. Soc.* **2002**, *124*, 760.
(53) Georgakilas, V.; Tagmatarchis, N.; Pantarotto, D.; Bianco, A.; Briand, J.-P.; Prato, M. *Chem. Commun.* **2002**, 3050.
(54) Kordatos, K.; Da Ros, T.; Bosi, S.; Vázquez, E.; Bergamin, M.; Cusan, C.; Pellarini, F.; Tomberli, V.; Baiti, B.; Pantarotto, D.; Georgakilas, V.; Spalluto, G.; Prato, M. *J. Org. Chem.* **2001**, *66*, 4915.
(55) Swali, V.; Wells, N. J.; Langley, J.; Bradley, M. *J. Org. Chem.* **1997**, *62*, 4902.
(56) Sarin, V. K.; Kent, S. B. H.; Tam, J. P.; Merrefield, R. B. *Anal. Biochem.* **1981**, *117*, 147.
(57) Tamiaki, H.; Suzuki, S.; Maruyama, K. *Bull. Chem. Soc. Jpn.* **1993**, *66*, 2633.

Scheme 1 [a]

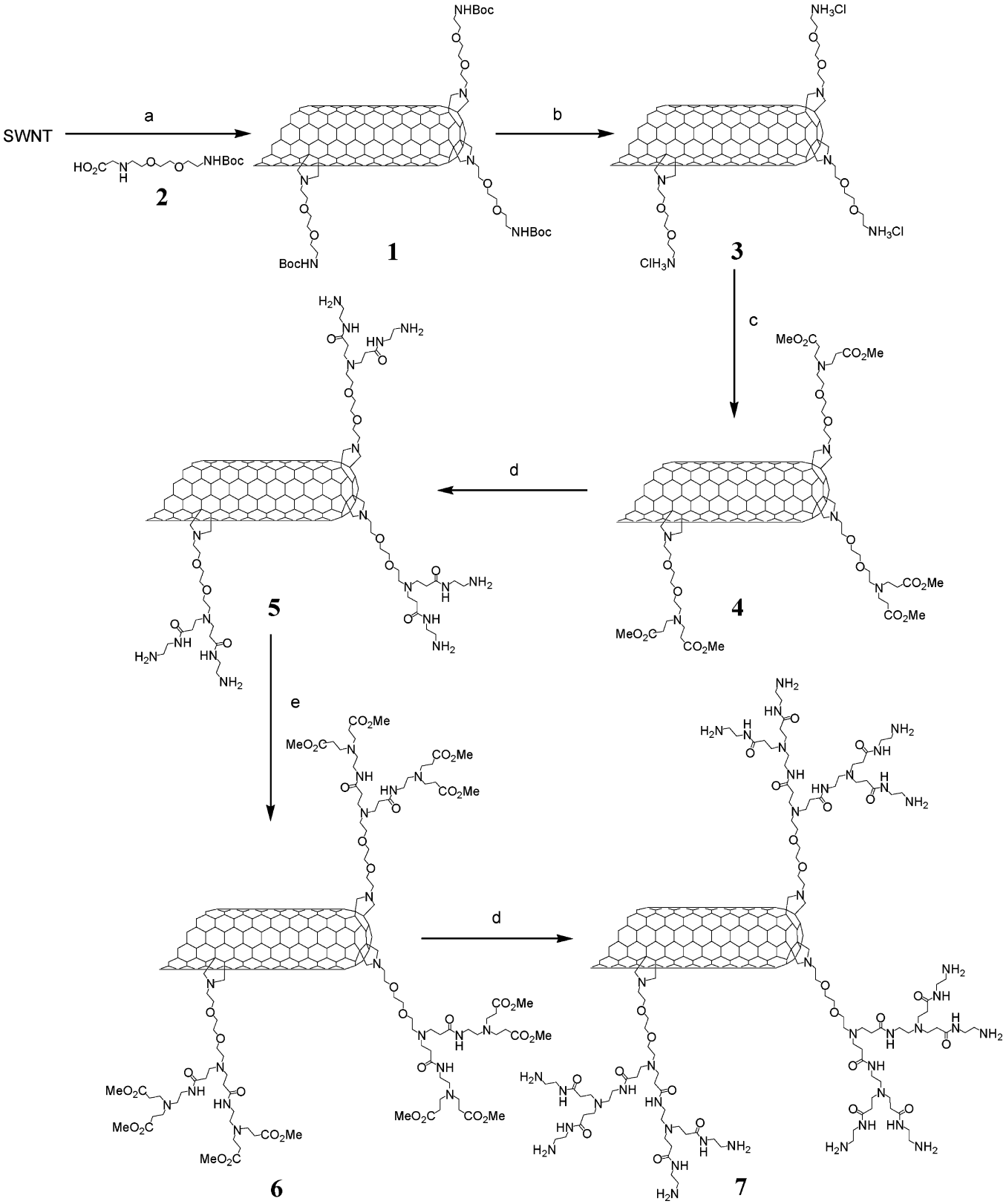

[a] Reagents and conditions: (a) paraformaldehyde, DMF, 120 °C, 5 days; (b) HCl gas, DMF, room temperature, 1 h; (c) methyl acrylate, *N*-ethyldiisopropylamine, MeOH, 80 °C, 3 days; (d) ethylenediamine, MeOH, 80 °C, 3 days; (e) methyl acrylate, MeOH, 80 °C, 3 days.

band at 1664 cm^{-1}, which corresponds to the stretching of the CO (carbamate) bond. This band disappears in compound **3**, where the *tert*-butyloxycarbonyl group has been removed. The IR spectra of the dendritic compounds **6**, **7**, and **9** present a series of peaks in the 1660−1730 cm^{-1} region (see the Experimental Section).

TGA of compounds **1** and **7** presents a loss of weight of about 13% and 33%, respectively, at 800 °C. This corresponds to the

Scheme 2 [a]

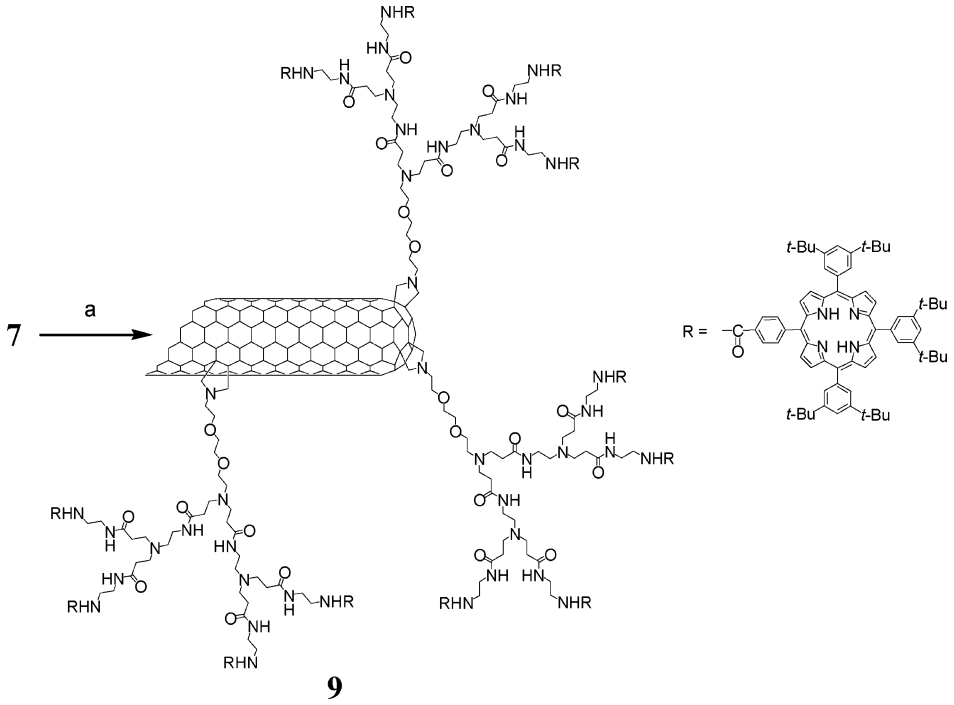

[a] Reagents and conditions: (a) porphyrin **8**, EDC, HOBt, DMF, room temperature, 5 days.

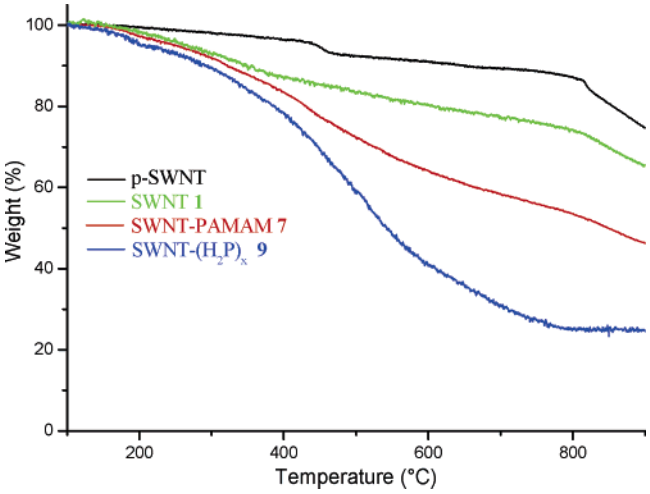

Figure 1. TGA of the pristine HiPCO SWNTs and nanotube derivatives **1**, **7**, and **9** (10 °C/min under N_2).

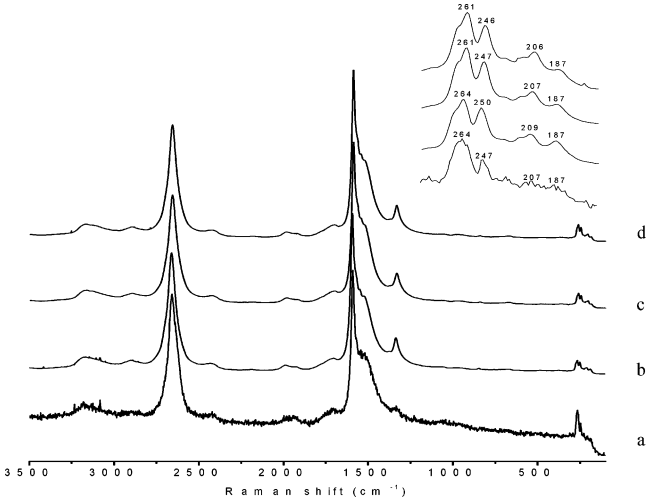

Figure 2. Raman spectra of the pristine SWNTs (a), functionalized nanotubes **1** (b), SWNT−PAMAM **7** (c), and SWNT−$(H_2P)_x$ **9** (d) at room temperature under dry air with an excitation wavelength of 514 nm.

presence of one functional group for about 140−150 carbon atoms in both cases (Figure 1). This result is in accordance with the structure and demonstrates that the dendrimer is formed at the surface of the nanotubes. The loss of weight of SWNT−$(H_2P)_x$ nanoconjugates **9** is about 62% at 800 °C. A simple calculation permits a loss of weight of 73% to be estimated if all amine groups of the dendrimers are connected to a porphyrin. Consequently, a weight loss of 62% indicates that not all amine groups have reacted, and we estimate that there is an average of two porphyrins on each dendrimer.

Raman Spectroscopy. Raman spectroscopy is a valuable tool to characterize nanotubes, because it provides detailed information on the structure and properties.[59] To avoid local heating during the data acquisition, the power of the laser was decreased to 5 mW at room temperature and 25 mW for the spectra taken at higher temperatures.

Figure 2 shows the Raman spectra of the pristine SWNTs as well as the functionalized nanotubes **1**, **7**, and **9** measured at room temperature under air. First, we observe an intensity increase of the signal at 1335 cm^{-1} (D band) in the functionalized nanotubes **1**—when compared to pristine SWNTs. This observation is not surprising, considering that we are adding functional groups covalently to the surface of the nanotubes.[35] Moreover, it is interesting to note that the D-band does not increase/decrease during the building of the dendrimer. This excludes further reactions at the nanotube sidewalls. Although it has been reported that amines can give rise to addition

(58) Luo, C.; Guldi, D. M.; Imahori, H.; Tamaki, K.; Sakata, Y. *J. Am. Chem. Soc.* **2000**, *122*, 6535.

(59) Dresselhaus, M. S.; Dresselhaus, G.; Saito, R.; Jorio, A. *Phys. Rep.* **2005**, *409*, 47.

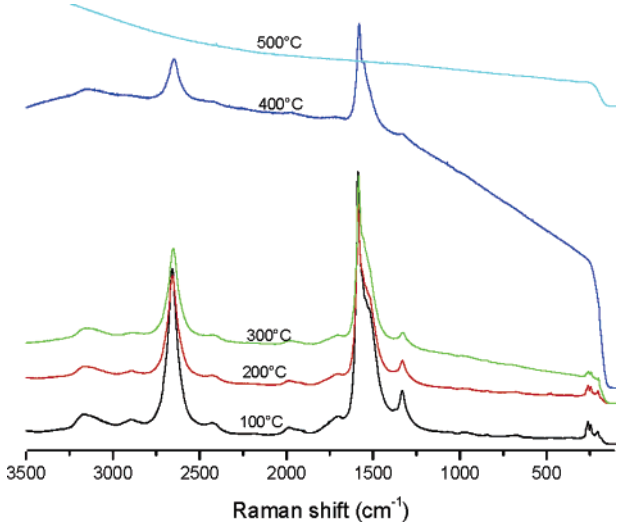

Figure 3. Thermal stability of SWNT−PAMAM **7**: Raman spectra at 100−500 °C with a ramp of 10 °C/min under dry air with an excitation wavelength of 514 nm. The nanotubes are stable until 300 °C; after this temperature the decomposition of the structure is clearly visible.

reactions to MWNTs,[60] this reaction does not seem to occur on our functionalized nanotubes probably because all the reactive sites are saturated with pyrrolidine rings.

Next, we focused our spectroscopic analysis on low-wavenumber phonon modes—radial breathing modes (RBMs). RBMs are very susceptible to the nanotube diameter and structure.[61,62] With excitation at 514 nm, the RBM bands are observed at room temperature at 264, 247, 207, and 187 cm^{-1} in all compounds—inset of Figure 2. The intensity of the peak centered at 264 cm^{-1} is significantly higher for the pristine material than for the functionalized material. On the contrary, the peaks at 207 and 187 cm^{-1} are hardly discernible in the raw material, but clearly appear after the functionalization. Such results might imply that, after the reaction, the mixture is enriched in nanotubes with bigger diameters.

It is interesting to compare the thermal stability of the modified SWNTs observed by TGA with the Raman spectra taken at variable temperatures.[63,64] Figure 3 shows the temperature analysis of the functionalized SWNT−PAMAM **7**. Already at 200 °C a significant decrease of the D-band is discernible, which becomes more evident at 300 °C. At 400 °C the D-band has nearly completely disappeared, in agreement with TGA data (vide supra). The fact that the original Raman bands are not recovered after heating to 500 °C indicates a gradual decomposition of the nanotube structure.

Microscopy. TEM confirmed the presence of SWNTs in our samples. Two representative images of nanoconjugates **7** and **9**, shown in Figure 4, reveal high-aspect-ratio objects that appear throughout the scanned regions. The mean length of these objects is typically on the order of several micrometers, and their diameters range between a few nanometers and several tens of nanometers. In this regard, the dendritic derivatives are different from pristine HiPCO SWNTs, in which aggregation

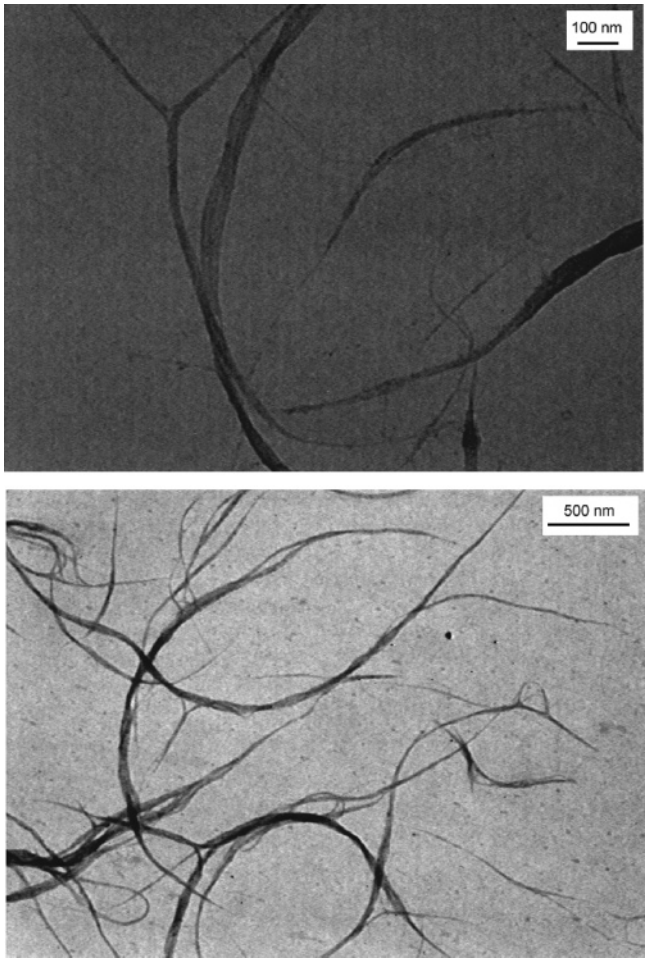

Figure 4. TEM images of the SWNT nanoconjugates **7** (top) and **9** (bottom) from a DMF solution.

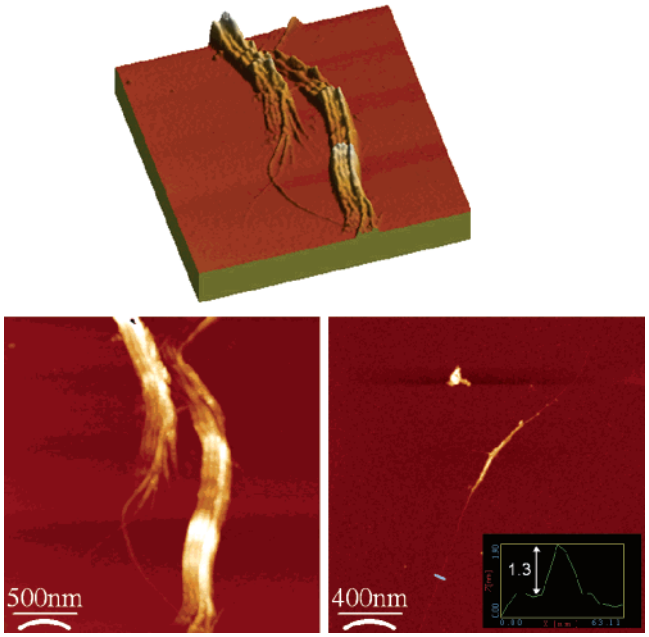

Figure 5. AFM images of SWNT−$(H_2P)_x$ nanoconjugate **9** prepared by spin coating on a silicon wafer from a DMF solution. The image on the left shows small aggregates, while on the right the image presents a very thin bundle ended by an individual carbon nanotube.

(60) Basiuk, E. V.; Monroy-Peláez, M.; Puente-Lee, I.; Basiuk, V. A. *Nano Lett.* **2004**, *4*, 863.
(61) Dresselhaus, M. S.; Dresselhaus, G.; Jorio, A.; Souza Filho, A. G.; Pimenta, M. A.; Saito, R. *Acc. Chem. Res.* **2002**, *35*, 1070.
(62) Dresselhaus, M. S.; Dresselhaus, G.; Jorio, A.; Souza Filho, A. G.; Saito, R. *Carbon* **2002**, *40*, 2043.
(63) Huong, P. V.; Cavagnant, R.; Ajayan, P. M.; Stephan, O. *Phys. Rev. B* **1995**, *51*, 10048.
(64) Iliev, M. N.; Litvinchuk, A. P.; Arepalli, S.; Nikolaev, P.; Scott, C. D. *Chem. Phys. Lett.* **2000**, *316*, 217.

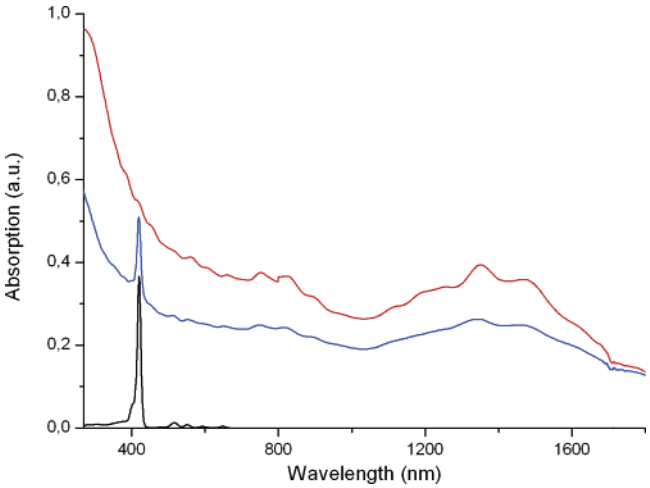

Figure 6. Absorption spectra of porphyrin **8** (black line), SWNT−PAMAM **7**, and SWNT−$(H_2P)_x$ nanoconjugate **9** in DMF.

prevents the observation of individual SWNTs or very thin bundles.

The nanoconjugates **7** and **9** have also been investigated by AFM. The samples were prepared by spin coating on a silicon wafer from a DMF solution and revealed in both cases the coexistence of individual SWNTs (diameters of around 1.3 nm) of several hundred nanometers in length and well-dispersed thin bundles of SWNTs (Figure 5).

Photophysical Properties. Absorption spectra of SWNT−$(H_2P)_x$ nanoconjugate **9** provide unquestionable evidence of the presence of both constituents, namely, SWNTs and H_2P. Figure 6 shows the Soret band of H_2P **8** at 419 nm, while the Q-band features are barely visible, since they are masked by the van Hove singularities of the SWNTs.[65] The van Hove singularities of the SWNTs are seen throughout the recorded range, that is, between 400 and 2200 nm. An important conclusion of the absorption features is that the electronic structure of the SWNTs is largely preserved.

The excited-state interactions were tested upon matching the absorption of SWNT−$(H_2P)_x$ nanoconjugate **9** at 419 nm with that of H_2P **8**, both in THF. In particular, fluorescence spectroscopy reveals a notable quenching (~85%) of the H_2P-centered features at 650 and 715 nm. In Figure 7 the uncorrected fluorescence spectra of SWNT−$(H_2P)_x$ and H_2P are compared.[66] We followed complementary to the steady-state fluorescence the fluorescence decay of the porphyrin at 650 nm by time-resolved means. For H_2P **8** a fluorescence lifetime of 9.5 ± 0.5 ns was registered. In SWNT−$(H_2P)_x$ **9**, on the other hand, the fluorescence decay (i.e., 650 and 715 nm) was best fitted by a biexponential function: a very short-lived (i.e., 0.04 ± 0.01 ns) and a long-lived (i.e., 8.6 ± 1.2 ns) component. The long-lived component bears great resemblance to that seen for H_2P. A possible rationale implies that H_2P chromophores do not interact with the SWNTs, due to the dendritic structure of $(H_2P)_x$. Interestingly, the preexponential factors of both components suggest a 9:1 ratio between the short- and long-lived parts.

Time-resolved transient absorption spectroscopy—following 150 fs and 6 ns laser excitation at 387 and 355 nm, respectively—

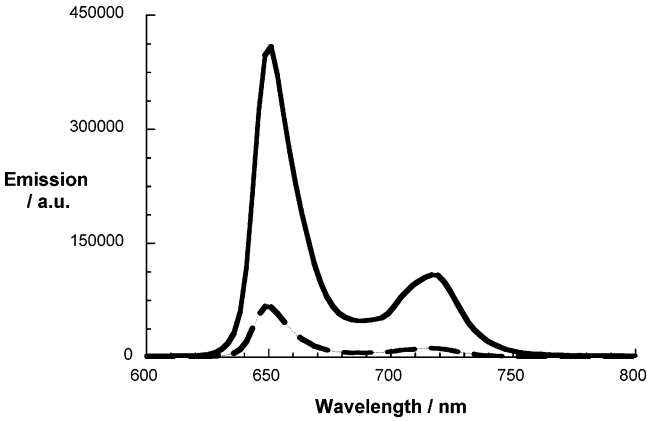

Figure 7. Room-temperature fluorescence spectra of H_2P **8** (solid line) and SWNT−$(H_2P)_x$ nanoconjugate **9** (dashed line) in THF with matching absorption at the 419 nm excitation wavelength.

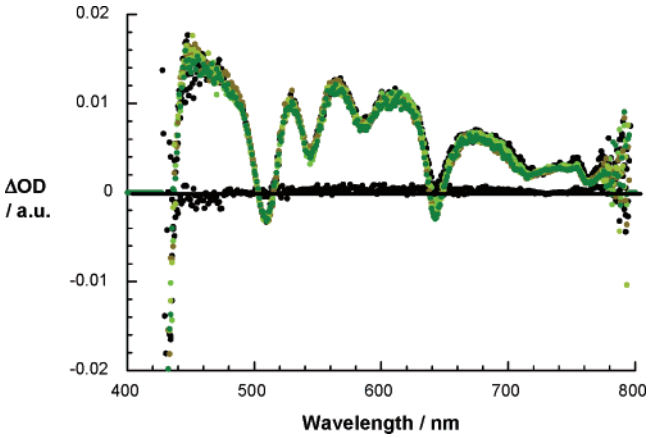

Figure 8. Differential absorption spectra (visible) obtained upon femtosecond flash photolysis (387 nm) of H_2P **8** in THF with several time delays between 0 and 200 ps at room temperature.

shed light onto the fate of photoexcited H_2P in the reference **8** and in the SWNT−$(H_2P)_x$ nanoconjugate **9**. The photophysics of H_2P are well established and have been reported by us on several occasions.[67,68] In short, the singlet excited state converts only slowly (i.e., 10.2 ± 0.5 ns) to the oxygen-sensitive triplet excited state. For illustration the singlet−singlet features, which include transient bleaching at 430, 510, 545, 585, and 645 nm, are depicted in Figure 8.

Initially, upon photoexcitation of SWNT−$(H_2P)_x$ nanoconjugate **9**, transient absorption changes are seen that resemble in the visible part those of the H_2P singlet excited state: minima at 415, 505, 545, 585, and 645 nm. This is fundamental, since it confirms the photoexcitation of the porphyrin in SWNT−$(H_2P)_x$. In the near-infrared part, features are noted that correspond to the SWNTs. Both parts are combined in Figure 9. The detailed analysis of the kinetic absorption time profiles reveals that the H_2P singlet excited state is short-lived—on the time scale of our femtosecond experiments—and converts rapidly into a new product. Kinetic analysis of the visible part, for which a few representative cases are gathered in Figure 9, gives a decay rate constant of (1.5 ± 0.5) × 10^{10} s^{-1} for the deactivation of the photoexcited H_2P. Such a value agrees well with the short-

(65) Strano, M. S.; Dyke, C. A.; Ursey, M. L.; Barone, P. W.; Allen, M. J.; Shan, H. W.; Kittrell, C.; Hauge, R. H.; Tour, J. M.; Smalley, R. E. *Science* **2003**, *301*, 1519.
(66) Implicit in "uncorrected" is that the competitive light absorption between the SWNTs and H_2P is not accounted for.
(67) Guldi, D. M. *Chem. Soc. Rev.* **2002**, *31*, 22.
(68) Guldi, D. M.; Rahman, G. M. A.; Sgobba, V.; Ehli, C. *Chem. Soc. Rev.* **2006**, *35*, 471.

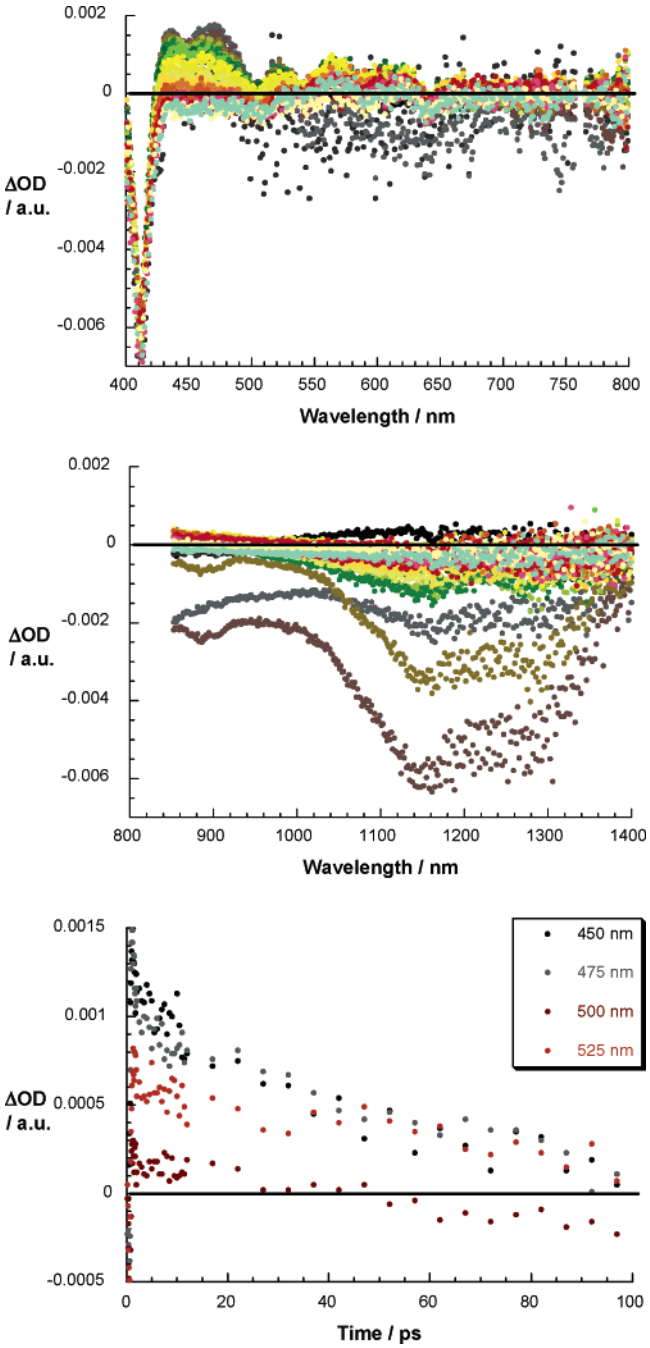

Figure 9. Upper part: differential absorption spectra (visible) obtained upon femtosecond flash photolysis (387 nm) of SWNT−$(H_2P)_x$ nanoconjugate **9** in THF with several time delays between 0 and 200 ps at room temperature. Middle part: differential absorption spectra (near-infrared) obtained upon femtosecond flash photolysis (387 nm) of SWNT−$(H_2P)_x$ nanoconjugate **9** in THF with several time delays between 0 and 200 ps at room temperature. Lower part: time−absorption profiles of the spectra shown above at 450, 475, 500, and 525 nm, monitoring the formation of the radical ion pair state.

lived component seen in the fluorescence studies. Notably, 387 nm photoexcitation of SWNT−$(H_2P)_x$ nanoconjugate **9** also directs a significant portion of the photons to the SWNTs. In line with this assumption we see the instantaneous (i.e., not resolved by the time resolution) bleaching of the SWNT van Hove singularities in the near-infrared part. When comparing the visible (i.e., 400−800 nm) and near-infrared (i.e., 900−1400 nm) parts, we noted notably different kinetics. The near-infrared part reveals composite kinetics that are due to either electron transfer evolving from photoexcited H_2P or photoexcited decay of SWNTs.

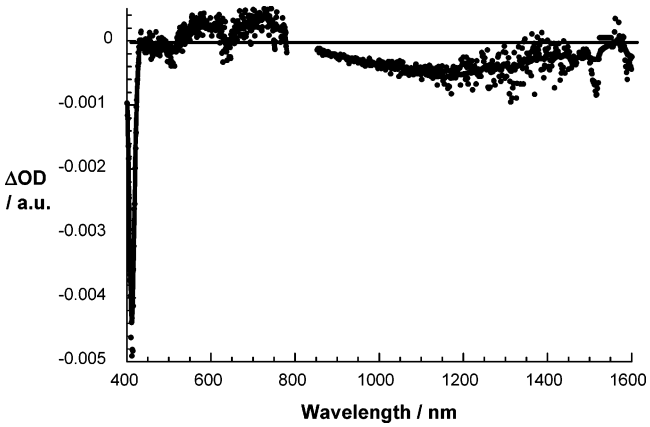

Figure 10. Differential absorption spectra (visible and near-infrared) obtained upon femtosecond flash photolysis (387 nm) of SWNT−$(H_2P)_x$ nanoconjugate **9** in THF with a time delay of 1500 ps at room temperature.

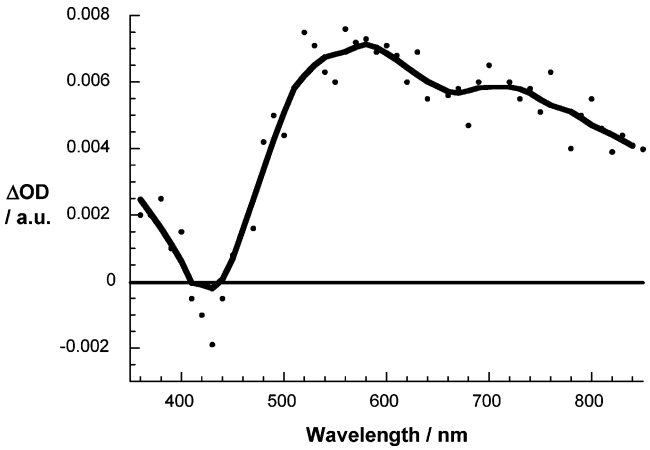

Figure 11. Differential absorption spectra (visible and near-infrared) obtained upon nanosecond flash photolysis (355 nm) of SWNT−$(H_2P)_x$ nanoconjugate **9** in THF with a time delay of 50 ns at room temperature.

The transient of the photoproduct is illustrated in Figure 10. One important feature is the broad absorption between 550 and 800 nm. Please note that the one-electron-oxidized product of H_2P shows similarly looking absorption characteristic.[69] A second feature is the transient bleach in the near-infrared region. In fact, the bleach appears as a mirror image of the ground-state absorption; compare Figures 6 and 10. In recent work bleaching of the van Hove singularities has been correlated with the reductive charging of SWNTs.[12] Considering all the above in concert, we postulate that the rapid decay of the H_2P singlet excited state is linked to an intraconjugate electron-transfer process. Features in both regions (i.e., visible and near-infrared) are stable on a time scale of up to 1500 ps.

In transient absorption measurements, where nanosecond laser pulses are utilized, a similarly looking radical ion pair spectrum is seen—Figure 11. The differential absorption changes decay to the baseline (i.e., ground state) with a major component that gives rise to kinetics of $(2.9 \pm 0.5) \times 10^6$ s^{-1}.

(69) Rodriguez, J.; Kirmaier, C.; Holten, D. *J. Am. Chem. Soc.* **1989**, *111*, 6500.

Conclusion

We have described the synthesis, characterization, and properties of a series of SWNTs functionalized with PAMAM dendrimers. The dendrimers were built directly onto the nanotube surface using a divergent methodology. Such an approach guarantees an increase of the functional groups on the nanotubes without causing significant damage to the electronic properties of the nanotubes. The dendrimers present on the nanotube sidewalls have been further functionalized with 5,10,15-tris(3,5-di-*tert*-butylphenyl)-20-[4-(carbonyloxy)phenyl]-porphyrins.

In response to visible light irradiation, SWNT−$(H_2P)_x$ nanoconjugate **9** gives rise to fast charge separation—$(1.5 \pm 0.5) \times 10^{10}$ s^{-1}—evolving from the photoexcited H_2P chromophores. Time-resolved fluorescence and transient absorption measurements were employed to corroborate this pathway. Most importantly, the oxidized H_2P chromophore was identified through its fingerprint absorption in the 550−800 nm range, while the signature of the reduced SWNTs appears in the 850−1400 nm range.

The addition of dendrimers to the nanotubes and their following treatment produce an enrichment of nanotubes of bigger diameter as shown by Raman spectroscopy.

We demonstrate here that dendrimers permit the number of photoactive groups on the surface of the nanotubes to be increased. The dendrimers with their porphyrins play conceptually the role of an antenna: harvesting light to give more efficient electron transfers.

It is known that [60]fullerene is a fantastic core for construction of dendrimers since its spherical shape gives rise to globular dendrimers even with low-generation dendrons. It is expected that attachment of dendrimers on carbon nanotubes may lead to cylinder-like objects with nanometer dimensions.

Experimental Section

Techniques. UV−vis−NIR spectra were recorded in 1 cm quartz cuvettes on a Varian Cary 5000 UV−vis−NIR spectrophotometer. The thermogravimetric analyses were performed with a TGA Q500 (TA Instruments) at 10 °C/min under N_2. FTIR spectra were recorded on a Thermo Nicolet Avatar 320 FT-IR spectrometer. The Raman spectra were run with a single monochromator Renishaw System 1000 equipped with a cooled CCD detector (−73 °C) and holographic super-Notch filter. The holographic Notch filter removes the elastic scattering. The samples were excited with the 514 nm Ar line; spectral resolution was ca. 3 cm^{-1}. The in situ Raman spectra were run under a dry air stream (40 mL/min) for the sample in a commercial hot stage (Linkam TS-1500). The sample was heated, and spectra were taken isothermally, 10 °C/min heating rate. The laser power on the sample was 25 mW, except in hydrated conditions (room temperature), in which it was only 5 mW to avoid dehydration for action of the laser. The signal-to-noise ratio was good with acquisitions adjusted to 20 scans of 20 s (or as indicated otherwise). Spectra were taken at constant temperature. To study thermal stability, samples were heated to 500 °C stepwise, 100 °C step and 10 °C/min heating rate, and next cooled to room temperature at a 10 °C/min rate, and a new spectrum was recorded. For the TEM analyses, a small amount of the functionalized SWNTs was suspended in DMF and a drop of the suspension was placed on a copper grid (3.00 mm, 200 mesh, coated with carbon film). After air-drying, the sample was investigated with a TEM Philips EM 208, accelerating voltage of 100 kV. For the AFM analyses, the samples were prepared by spin coating on silicon wafers from a solution of SWNTs in DMF and then investigated with a Veeco Multimode scanning probe microscope equipped with a Nanoscope IIIa controller.

Photophysical Measurements. Femtosecond transient absorption studies were performed with 387 nm laser pulses (1 kHz, 150 fs pulse width) from an amplified Ti:sapphire laser system (model CPA 2101, Clark-MXR Inc.). Nanosecond laser flash photolysis experiments were performed with 532 nm laser pulses from a Quanta-Ray CDR Nd:YAG system (6 ns pulse width) in a front face excitation geometry. For all photophysical experiments an error of 10% must be considered. Fluorescence lifetimes were measured with a laser strobe fluorescence lifetime spectrometer (Photon Technology International) with 337 nm laser pulses from a nitrogen laser fiber coupled to a lens-based T-formal sample compartment equipped with a stroboscopic detector. Details of the laser strobe systems are described on the manufacturer's Web site, http://www.pti-nj.com. Emission spectra were recorded with an SLM 8100 spectrofluorometer.

Materials. HiPCO SWNTs were purchased from Carbon Nanotechnologies Inc. (www.cnanotech.com). Solvents and chemicals were purchased form Aldrich and were used as received. Compounds **2**[54] and **8**[57,58] were synthesized following literature procedures.

Synthesis. SWNTs 1. A suspension of SWNTs (100 mg) in dry DMF (200 mL) was first sonicated for 30 min, then amino acid **2** (600 mg) and paraformaldehyde (600 mg) were added portionwise (150 mg every 24 h), and the reaction mixture was heated at 120 °C for 5 days. After being cooled to room temperature (rt), the suspension was sonicated and centrifugated. The solution was filtered on a Millipore membrane (PTFE, 0.22 μm), and the black solid was washed several times with fresh DMF (sonicated, centrifugated, and filtered) until the supernatant solution remained colorless. The solid on the filter was washed with CH_2Cl_2 and diethyl ether, affording functionalized SWNTs **1** (27 mg). FT-IR (KBr): ν (cm^{-1}) 2919, 2853, 1664, 1444, 1378, 1075, 1024.

SWNTs 3. Into a suspension of SWNTs **1** (25 mg) in dry DMF (100 mL) was bubbled gaseous HCl, and the nanotubes immediately started to precipitate. The reaction mixture was stirred at room temperature for 2 h and then filtered on a Millipore membrane (PTFE, 0.22 μm), and the solid on the filter was washed with CH_2Cl_2 and diethyl ether. After drying under vacuum, SWNTs **3** were obtained as a black solid (25 mg). FT-IR (KBr): ν (cm^{-1}) 2925, 2850, 1590, 1443, 1383, 1017.

SWNTs 4. To a suspension of SWNTs **3** (20 mg) in dry methanol (10 mL) were added *N*-ethyldiisopropylamine (2 mL) and methyl acrylate (10 mL). The reaction mixture was stirred at 80 °C for 3 days and then filtered on a Millipore membrane (PTFE, 0.22 μm), and the solid on the filter was washed with CH_2Cl_2 and diethyl ether. SWNTs **4** were obtained as a black solid (20 mg). FT-IR (KBr): ν (cm^{-1}) 2924, 2853, 1733, 1664, 1596, 1443, 1383, 1022.

SWNTs 5. To a suspension of SWNTs **4** (20 mg) in dry methanol (10 mL) was added ethylenediamine (10 mL). The reaction mixture was stirred at 80 °C for 3 days and then filtered on a Millipore membrane (PTFE, 0.22 μm), and the solid on the filter was washed with CH_2Cl_2 and diethyl ether. SWNTs **5** were obtained as a black solid (22 mg). FT-IR (KBr): ν (cm^{-1}) 2924, 2853, 1661, 1596, 1443, 1378.

SWNTs 6. To a suspension of SWNTs **5** (10 mg) in dry methanol (10 mL) was added methyl acrylate (10 mL). The reaction mixture was stirred at 80 °C for 3 days and then filtered on a Millipore membrane (PTFE, 0.22 μm), and the solid on the filter was washed with CH_2Cl_2 and diethyl ether. SWNTs **6** were obtained as a black solid (10 mg). FT-IR (KBr): ν (cm^{-1}) 2919, 2858, 1716, 1667, 1590, 1443, 1378, 1181, 1006.

SWNTs 7. To a suspension of SWNTs **6** (10 mg) in dry methanol (10 mL) was added ethylenediamine (10 mL). The reaction mixture was stirred at 80 °C for 3 days and then filtered on a Millipore membrane (PTFE, 0.22 μm), and the solid on the filter was washed with CH_2Cl_2 and diethyl ether. SWNTs **7** were obtained as a black solid (11 mg). FT-IR (KBr): ν (cm^{-1}) 2924, 2853, 1700, 1678, 1552, 1514, 1055, 1001.

SWNTs 9. To a suspension of SWNTs **7** (5 mg) in dry DMF (10 mL) were added the free base porphyrin **8** (10 mg), EDC (100 mg), and HOBt (100 mg). The reaction mixture was stirred at room temperature for 5 days and then filtered on a Millipore membrane (PTFE, 0.22 μm), and the solid was washed with DMF, CH_2Cl_2, and diethyl ether. SWNTs **9** were obtained as a black solid (6 mg). FT-IR (KBr): ν (cm^{-1}) 2924, 2853, 1700, 1651, 1558, 1508, 1197, 1066.

Acknowledgment. This work was carried out with partial support from the University of Trieste, MIUR (PRIN 2004, prot. 2004035502, and Firb RBNE033KMA), EU (RTN network "WONDERFULL"), the Swiss National Science Foundation (Grant No. PBNE2-106767), SFB 583, DFG (Grant GU 517/4-1), FCI, and the Office of Basic Energy Sciences of the U.S. Department of Energy (NDRL 4687). E.L.D. thanks the Comunidad Autonoma de Madrid, Spain (Grant No. GR/AMB/0751/2004).

JA063697I